available at www.sciencedirect.com

ScienceDirect

journal homepage: www.elsevier.com/locate/jhydrol

Hydrogeochemical and isotopic investigations of the Han River basin, South Korea

Jong-Sik Ryu [a,b], Kwang-Sik Lee [a,*], Ho-Wan Chang [b]

[a] *Korea Basic Science Institute, 52 Eoeun-dong, Yusung-gu, Daejeon 305-333, Republic of Korea*
[b] *School of Earth and Environmental Sciences, Seoul National University, Seoul 151-742, Republic of Korea*

Summary The Han River, the largest river in South Korea draining approximately 26,000 km^2, comprises two major tributaries: the North and the South Han Rivers. Seasonal and spatial variations in the major ion chemistry and isotope compositions of the Han River were monitored for one year at 14–23 locations, covering about 80% of the entire drainage basin. Compared to the South Han River (SHR), the North Han River (NHR) was much lower in total dissolved solids (TDS), Sr, and major ion concentrations, but higher in Si concentration, $\delta^{34}S_{SO_4}$ values, and $^{87}Sr/^{86}Sr$ ratios. These observations suggest strong influence of prevailing rock types in the drainage basins on the chemical and isotopic compositions of the river waters. These are silicate rocks in the NHR basin and carbonate rocks in the SHR basin. The headwaters of the NHR basin, where several flood control dams have been constructed, show enrichment in deuterium and oxygen-18, indicating evaporative loss. The $\delta^{34}S_{SO_4}$ data suggest dissolved sulfates in the NHR and SHR are mostly derived from atmospheric deposition, and variable mixtures of atmospheric deposition and sulfide oxidation, respectively. The $^{87}Sr/^{86}Sr$ ratios are much higher in the NHR (0.71793–0.72722) than in the SHR (0.71495–0.71785) with one exception, indicating weathering of Precambrian and Mesozoic granitic rocks and marine carbonates, respectively.
© 2007 Elsevier B.V. All rights reserved.

Introduction

River transports weathering products from continents to oceans and chemical and isotopic compositions of river waters can provide useful information on the sources of dissolved loads, extent of chemical weathering in the drainage basins, and terrestrial fluxes to oceans. Many studies on major rivers around the world have focused on characterizing the source rocks (carbonates and silicates) that control water chemistry in their basins (e.g. Stallard and Edmond, 1987; Amiotte-Suchet and Probst, 1993; Négrel and Dupré, 1995; Petelet et al., 1998; Gaillardet et al., 1999; Karim and Veizer, 2000; Viers et al., 2000; Quade et al., 2003; Han and Liu, 2004; Wu et al., 2005; Moon et al., 2006; Qin et al., 2006; Xu and Liu, 2007). These studies reveal that rel-

ative to silicate weathering carbonate weathering dominates river water chemistry.

Major rivers in South Korea include the Han River, Geum River, Sumjin River, Nakdong River, and Yeongsan River. Of these rivers, the Han River, which comprises the North Han River (NHR), South Han River (SHR), and many small tributaries (Fig. 1), has the largest drainage basin. The NHR basin lies on the Precambrian gneisses and Mesozoic granites, and the SHR drains Paleozoic carbonates and clastic sedimentary rocks (Chough et al., 2000). Such a striking difference between the rock types of the NHR and SHR basins provides a good example for investigating the impact of weathering processes and rock types on river water chemistry.

In spite of the socio-economic importance of the Han River as a major source of drinking water supply to more than 20 million inhabitants in the central Korean Peninsular, no watershed-scale information is available on the chemical and isotopic characteristics of the rivers. Only a few studies have investigated local hydrochemistry and isotopic compositions (Mizutani et al., 1982; Yu et al., 1994; Lee and Lee, 1999; Chae et al., 2004).

This study investigates on a watershed-scale, the seasonal and spatial variations of chemical and isotopic compositions of the Han River waters and the constraints on water–rock interactions to determine the processes and factors controlling the river water chemistry. These observations are then compared with the major river systems in China. This study will provide baseline information on the overall characteristics of the Han River water chemistry and provide a basis for future watershed-scale investigations on other major rivers in Korea.

The Han River basin characteristics

The Han River consists of two major tributaries (the NHR and SHR) and many small tributaries (Fig. 1). It drains an area of 26,018 km^2 or 27% of South Korea and is 5417 km long (KOWACO, 1993). The annual discharge varies between

Figure 1 A simplified geological map of the Han River basin showing sampling locations. The inset shows location of the study area.

16.0 and 18.9 km^3. The river originates at an altitude of more than 1300 meters above sea level in the Taeback Mountains, and traverses the mid-western parts of the Korean Peninsula before flowing into the Yellow Sea. Much of the river catchments are in mountainous terrain. The two tributaries of the Han River join at the Paldang dam, forming the main channel (Fig. 1). The Paldang dam is the first reservoir located on the main river channel and serves as a reference point for sampling campaigns in this study.

The climate of the study area is temperate with four different seasons. The monthly average temperatures in the study area varied from −2.5 °C in January to +25.4 °C in August. The 30-year (1971–2000) average annual precipitation is 1344 mm, and about two-thirds of the annual precipitation occurs between June and September (Korea Meteorological Administration, website: www.kma.go.kr).

Fig. 1 shows a simplified geological map of the Han River basin. The NHR basin mainly consists of Precambrian gneisses and Mesozoic granites, whereas Ordovician limestones and Permo-Carboniferous coal-bearing clastic sedimentary rocks are widely distributed in the upper part of the SHR basin. Limestones are locally metasomatized by the Mesozoic granites. Numerous polymetallic skarn deposits are developed along contact zones. A recent study on the carbon isotopic contents of dissolved inorganic carbon ($\delta^{13}C_{DIC}$) suggests that the $\delta^{13}C_{DIC}$ values of the SHR and NHR are constrained by input of sedimentary carbonates and oxidation of soil organic materials, respectively (Lee et al., 2007).

Sampling and analytical methods

To investigate the seasonal and spatial variations of hydrochemical and isotopic compositions of the Han River basin, water samples were collected from 14 to 23 sites during three sampling campaigns carried out in August 2000 (summer, high water stage), December 2000 (winter, low water stage) and March 2001 (spring, rising water stage). Sampling sites (Fig. 1) were selected to avoid any anthropogenic point source contaminations and direct influences of tributaries. Numbers and locations of samples varied during each sampling campaign due to accessibility and water regime. At each site, a water sample was taken from a consistent depth. Temperature, pH and electrical conductivity (EC) of water samples were measured in the field. Alkalinity was determined within 12 hours after sampling by Gran titration method using 0.1 N HCl.

Samples for chemical and Sr isotopic analysis were passed through 0.45 μm pre-cleaned membrane filters and kept refrigerated at approximately 4 °C before analyses. All analyses were done just after sampling was conducted. Samples for cation analysis were acidified in the field with ultrapure HNO_3 to a pH of <2. Cations were analyzed by ICP-MS, and ICP-AES at the Korea Basic Science Institute (KBSI). Internal standards (In, Rh and Tl) were used for the calibration of cation data. The analytical uncertainties range from 2 to 5% for major ions. Anions were analyzed by ion chromatography (Dionex DX-500 IC) at the Seoul National University.

For oxygen isotopic analysis, about 2 ml of each water sample was equilibrated with CO_2 gas at 25.0 ± 0.1 °C (Epstein and Mayeda, 1953). The CO_2 gas was then extracted
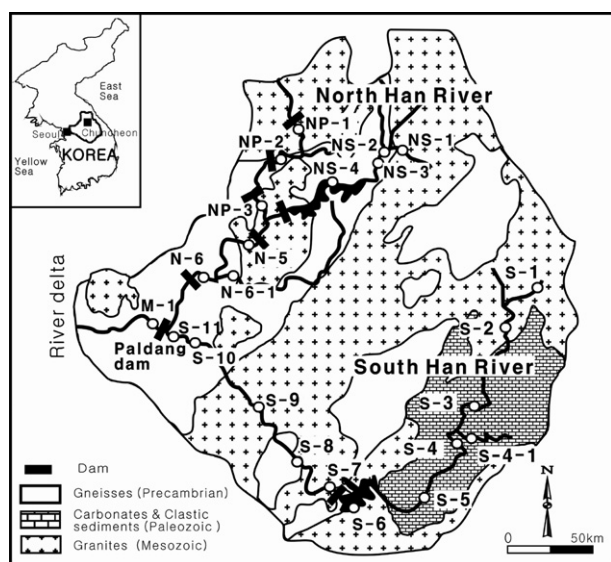
and cryogenically purified. For deuterium isotope analysis, metallic zinc was used to produce hydrogen gas (Coleman et al., 1982). For the analysis of $\delta^{34}S_{SO_4}$, sulfates were precipitated as $BaSO_4$ by adding a saturated $BaCl_2$ solution to the filtered water samples. SO_2 gas was then prepared as described by Yanagisawa and Sakai (1983). The oxygen, hydrogen and sulfur isotopic compositions of samples were determined using a VG Prism II stable isotope ratio mass spectrometer at the KBSI. Stable isotopic compositions are expressed in the usual δ notation relative to the V-SMOW for oxygen and hydrogen isotopes, and CDT for sulfur isotopes. $\delta(\permil) = (R_{sample}/R_{standard} - 1) \times 1000$, where R represents $^{18}O/^{16}O$, D/H, or $^{34}S/^{32}S$. The analytical reproducibilities for each standard are $\pm 0.1\permil$ for $\delta^{18}O$, $\pm 1\permil$ for δD and $\pm 0.2\permil$ for $\delta^{34}S$.

For Sr isotopic analysis, approximately 60 ml of each water sample was evaporated to dryness in ultraclean Teflon vessels and redissolved in distilled HCl. Strontium in the solution was then separated from other ions by cation exchange resin (BioRad® AG 50 W X8 200—400 mesh) in a quartz column. Total Sr blank level was less than 0.1 ng. Sr isotopes were determined using a VG54-30 thermal ionization mass spectrometer at the KBSI. The $^{87}Sr/^{86}Sr$ ratios were normalized to $^{86}Sr/^{88}Sr = 0.1194$, and the mean $^{87}Sr/^{86}Sr$ ratio of the NBS987 standard during analysis was 0.710247 ± 0.000008 (2σ, $n = 12$).

Results and discussion

General observation of water chemistry

The chemical compositions of the Han River and its tributaries are given in Table 1. The pH values of the river samples ranged from 7.61 to 8.98 with an average of 8.39. Spatially, a slight downriver increase in pH value (~ 1.1) was also observed. The average pH values were slightly higher in the SHR (8.62) than in the NHR (8.14) (Table 1). The pH values of water samples collected during spring and summer seasons are much higher than those collected during winter season. This may be attributed to the aquatic plankton blooms during warm season (Vedula and Medina, 2002). Elevated pH values of river waters may also result from local discharge of high-pH groundwaters. To address this problem in the study area, detailed hydrological and hydro-ecological studies are needed.

The total dissolved cations ($TZ^+ = Na^+ + K^+ + 2Mg^{2+} + 2\text{-}Ca^{2+}$) and total dissolved anions ($TZ^- = Cl^- + 2SO_4^{2-} + NO_3^- + HCO_3^-$) for most of the water samples were balanced to within $\pm 8\%$ of the normalized inorganic charge balance [NICB, defined as $(TZ^+\text{-}TZ^-)/TZ^+$] (Huh et al., 1998).

The total cation concentrations follow the order Ca > Na > Mg > K for the NHR and Ca > Mg > Na > K for the SHR. The TZ^+ values are in the range of 0.38—1.27 meq/l for the NHR and range between 0.29 and 2.56 meq/l for the SHR (Table 1). The TZ^+ values of the NHR draining granitic rocks are similar to the global river average ($TZ^+ = 0.725$ meq/l; Meybeck, 1988) and are within the range of the world's 62 largest rivers (Gaillardet et al., 1999). The TZ^+ values of the SHR draining karst terrains are, however, nearly three times higher than the global river average.

Sample S-1 taken from the pristine headwaters of the SHR during spring season yields the lowest TZ^+ value (0.29 meq/l), probably due to the existence of silicate basement. No carbonates have been found in this region. These observations indicate that the geochemical characteristics of the Han River waters are strongly constrained by the lithologies of the drainage basins. On the other hand, the chemistry of a pristine headwater draining silicates seems to be governed by atmospheric input and local groundwater discharge.

Bicarbonate (HCO_3^-) is the dominant anion, accounting for approximately 60—70% of TZ^- of most samples. HCO_3^- is much higher in the SHR (0.15—1.60 mmol/l) draining carbonate terrain than in the NHR (0.14—0.93 mmol/l) draining crystalline terrain (Table 1). Sample S-1 taken from the pristine headwaters draining silicate terrain is an exception. Our data are within the range of values (1.2—3.4 mmol/l) of the five major Chinese rivers draining silicate and carbonate terrains, and falls within range (0.2—4.2 mmol/l) of the world's 62 major rivers (Gaillardet et al., 1999; Han and Liu, 2004).

Sulfate (SO_4^{2-}) concentrations range from 0.04 to 0.09 mmol/l for the NHR and from 0.04 to 0.32 mmol/l for the SHR. Even though SO_4^{2-} content of precipitation was not measured in this study, our values in the NHR are within the range (0.01—0.15 mmol/l) reported in Yu and Park (2004). They attributed atmospheric input as the major source of SO_4^{2-} in the upper NHR basin. The origin of sulfate is discussed further with $\delta^{34}S$ data in Section ''Sulphur isotopes''.

Average nitrate (NO_3^-) concentrations are nearly two times higher in the SHR (0.15 ± 0.03 mmol/l, $n = 27$) than in the NHR (0.08 ± 0.026 mmol/l, $n = 25$), indicating possible inputs from agricultural sources in the SHR (Table 1).

Waters in the basin are of two hydrochemical types: Ca—Na—HCO_3 type for the NHR and Ca—Mg—HCO_3—SO_4 type for the SHR (Fig. 2). In the SHR the relatively high $Ca^{2+} + Mg^{2+}$ concentrations, accounting for $\sim 90\%$ of cations, and high Sr concentrations strongly indicate that the water chemistry is controlled by carbonate dissolution in its drainage basin. Samples from the Paldang dam plot around the boundary between the two water types. However, the Paldang water is not exactly on the boundary, indicating incomplete mixing of waters. Mixing calculations are described in more detail in Section ''Quantifying mixing of river waters at confluence point''.

Atmospheric input and anthropogenic effects

In order to discriminate the different weathering sources in a river system, the atmospheric contribution should be evaluated (Meybeck, 1983). The correction for atmospheric input consists of quantifying and subtracting the portion of ions contributed by rainwater. Chloride has been widely used as a tracer for evaluating the atmospheric input because it behaves conservatively in natural environments (Stallard and Edmond, 1981; Meybeck, 1983).

Because no rock salt or evaporite deposit has been reported in the Han River basin (Chough et al., 2000), we assume that chloride in the pristine headwaters (Sample NS-1) of the Han River is entirely derived from the atmosphere. However, in the middle and lower parts of the basin, a

Table 1 Physical and chemical properties of the Han River waters

Sample	pH	Temperature (°C)	TDS (mg/l)	Na (mmol/l)	Mg (mmol/l)	K (mmol/l)	Ca (mmol/l)	Si (mmol/l)	Sr (μmol/l)	Cl (mmol/l)	NO_3 (mmol/l)	SO_4 (mmol/l)	HCO_3 (mmol/l)	TZ^+ (meq/l)	TZ^- (meq/l)	n^a
Main channel of the Han River																
M-1	8.46	17.5	98.4	0.25	0.14	0.04	0.42	0.06	0.90	0.19	0.12	0.12	0.83	1.40	1.38	3
North Han River																
NS-1	7.61	11.1	26.0	0.11	0.03	0.01	0.10	0.14	0.22	0.06	0.07	0.04	0.14	0.38	0.38	3
NS-2	7.97	13.8	—	0.11	0.03	0.02	0.11	0.09	0.31	0.08	0.10	0.04	—	0.41	—	1
NS-3	8.32	11.6	45.8	0.14	0.05	0.02	0.15	0.10	0.51	0.10	0.09	0.05	0.33	0.57	0.64	2
NS-4	8.26	18.3	39.2	0.13	0.06	0.03	0.17	0.10	0.54	0.08	0.10	0.06	0.39	0.60	0.68	3
NP-1	7.81	12.3	73.1	0.12	0.18	0.03	0.38	0.07	0.55	0.08	0.06	0.09	0.93	1.27	1.24	2
NP-2	8.29	17.4	75.7	0.14	0.13	0.03	0.32	0.09	0.57	0.08	0.05	0.07	0.75	1.09	1.04	3
NP-3	7.81	14.8	69.0	0.14	0.12	0.03	0.30	0.08	0.56	0.09	0.06	0.07	0.65	1.00	0.94	3
N-5	8.01	14.7	53.4	0.16	0.09	0.03	0.23	0.09	0.54	0.10	0.08	0.06	0.51	0.82	0.81	3
N-6	8.73	17.3	51.7	0.17	0.08	0.03	0.21	0.09	0.55	0.10	0.08	0.06	0.49	0.78	0.80	3
N-6-1	8.59	11.4	68.9	0.37	0.09	0.04	0.27	0.04	0.88	0.20	0.12	0.09	0.62	1.13	1.11	2
Mean	**8.14**	**14.6**	**54.8**	**0.15**	**0.09**	**0.03**	**0.23**	**0.09**	**0.53**	**0.10**	**0.08**	**0.06**	**0.54**	**0.82**	**0.84**	**25**
South Han River																
S-1	8.50	16.3	17.9	0.08	0.03	0.01	0.07	0.10	0.25	0.05	0.05	0.04	0.15	0.29	0.32	1
S-2	8.98	11.5	125	0.14	0.17	0.02	0.62	0.05	1.35	0.15	0.16	0.14	1.16	1.75	1.75	2
S-3	8.63	15.4	164	0.13	0.28	0.03	0.92	0.05	2.76	0.15	0.17	0.32	1.60	2.56	2.55	3
S-4	8.64	16.0	171	0.15	0.29	0.03	0.86	0.04	2.01	0.15	0.17	0.24	1.57	2.47	2.38	3
S-4-1	8.82	8.8	138	0.07	0.18	0.02	0.72	0.04	0.87	0.10	0.15	0.15	1.36	1.89	1.92	2
S-5	8.43	16.2	161	0.14	0.26	0.03	0.82	0.05	1.57	0.13	0.16	0.21	1.51	2.31	2.23	3
S-6	8.47	12.2	140	0.13	0.21	0.03	0.68	0.02	1.18	0.14	0.16	0.16	1.31	1.96	1.93	2
S-7	8.44	17.9	143	0.14	0.24	0.06	0.73	0.02	1.32	0.16	0.15	0.18	1.39	2.14	2.06	3
S-8	8.76	12.9	175	0.26	0.24	0.04	0.76	0.01	1.32	0.19	0.16	0.24	—	2.29	—	1
S-9	8.60	18.6	145	0.25	0.21	0.04	0.68	0.04	1.24	0.19	0.13	0.16	1.35	2.07	2.00	3
S-10	8.78	13.2	139	0.33	0.23	0.05	0.69	0.02	1.29	0.28	0.16	0.21	1.41	2.21	2.27	2
S-11	8.42	13.3	127	0.35	0.21	0.05	0.66	0.03	1.24	0.25	0.14	0.18	1.30	2.14	2.05	2
Mean	**8.62**	**14.7**	**144.7**	**0.18**	**0.23**	**0.04**	**0.73**	**0.04**	**1.49**	**0.16**	**0.15**	**0.20**	**1.38**	**2.13**	**2.08**	**27**

—: Not analysed.
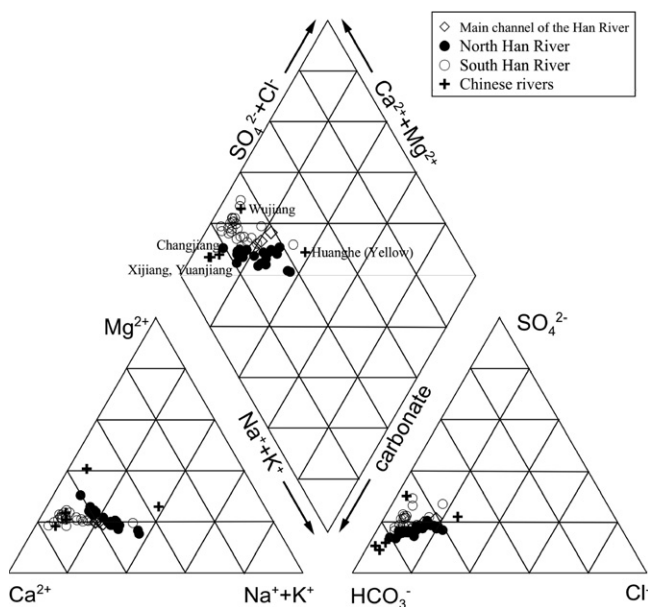
[a] Number of samples analyzed.

Figure 2 Piper diagram for hydrochemical types of the Han River. All data in meq/l normalized to 100%.

significant amount of chloride may originate from anthropogenic sources (manure, sewage, fertilizer, road salt, etc). This is represented by concentration spikes of chloride, sulfate and nitrate in downriver direction (Table 1). Concentrations of dissolved ions in river water samples were corrected using element/chloride ratios of local rain of Yu and Park (2004). The contribution of the atmospheric inputs to the dissolved loads in the NHR waters was estimated as 8—33% for TZ^+ and 15—35% for TZ^-, while in the SHR waters 4—7% for TZ^+ and 7—12% for TZ^-.
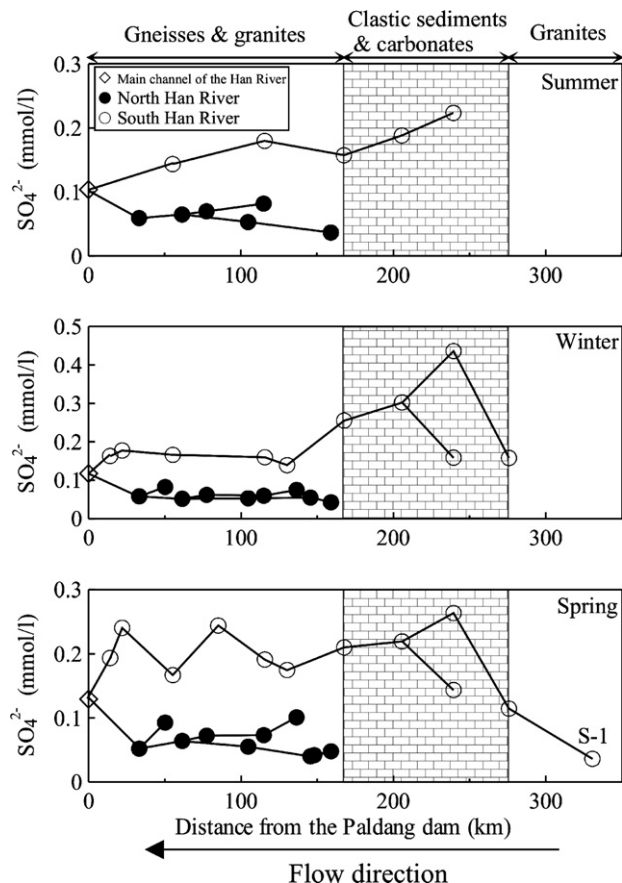
Figure 4 Temporal and spatial variations of sulfate concentrations in the Han River. Sulfate concentrations increase abruptly as waters flow through the sedimentary part of the basin.
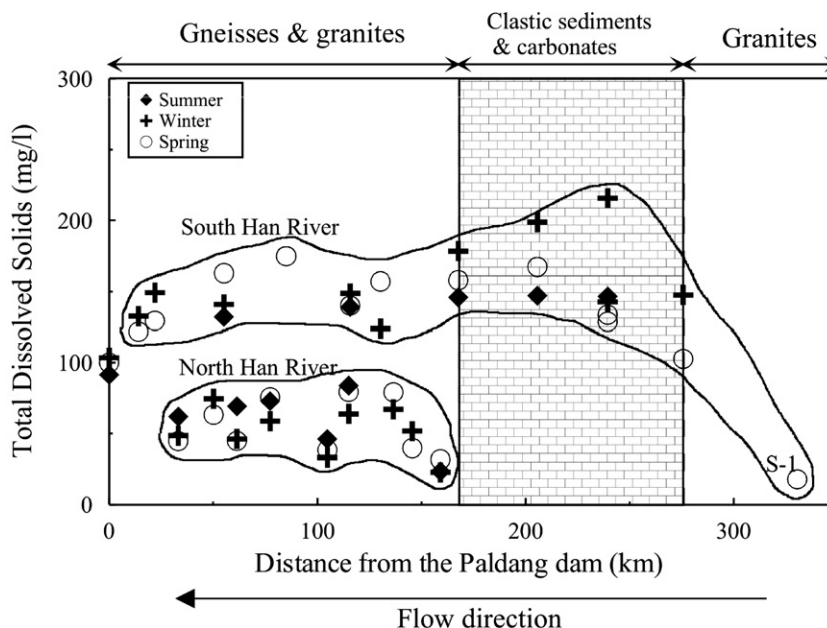

Figure 3 Temporal and spatial variations of total dissolved solids (TDS) in the Han River. In the South Han River basin, TDS values increase abruptly as waters flow through the carbonate section of the drainage basin.

In general, anthropogenic activity can easily modify the chemistry of rivers. In the Han River basin, the concentrations of nitrates and sulfates significantly increase as water flows through agricultural areas. In particular, the concentrations of nitrates and sulfates are much higher in the SHR (Table 1) draining more widespread agricultural regions relative to the NHR. This is likely due to the use of agricultural fertilizers. It seems that the SHR waters are more contaminated by anthropogenic inputs relative to the NHR waters.

Seasonal and spatial variations in water chemistry

Major ion concentrations and TDS of the Han River are variable in time and space, and are strongly influenced by tributaries and dams (Figs. 3 and 4). A striking difference is observed between TDS contents of the NHR and SHR (Table 1). Average TDS value of the SHR (148.7 ± 23.6 mg/l, $n = 26$) draining carbonate terrain except for a sample S-1 is nearly three times higher than that of the NHR (54.8 ± 17.9 mg/l, $n = 24$) draining a non-carbonate terrain (Fig. 4). The TDS value of sample S-1, taken from the SHR headwater in the spring, is the lowest (17.9 mg/l), probably due to slow weathering in granite basement and short residence time of water. The residence time of the Han River water is relatively short (less than a few months) (Han River Flood Control Office, website: www.hrfco.go.kr).

TDS values increase abruptly to 216 mg/l as water flows through the carbonate section of the drainage basin (Fig. 3). This observation suggests that water chemistry of the Han River is greatly influenced by the rock types of the drainage basin, i.e., carbonate weathering exerts a greater impact than silicate weathering.

Seasonal variations in TDS are observed in the upstream SHR, where there is no dam. TDS values are the lowest in the summer, indicating dilution due to heavy rain. The highest values are observed during the winter, indicating increased relative contribution from groundwater (Lee and Kim, 2007). However, these seasonal variations in TDS appear to be considerably attenuated or even reversed in the middle and downstream reaches of both rivers where several flood control dams enable mixing.

Sulfate concentrations show similar seasonal and spatial variations as TDS values (Fig. 4). Although no evaporite deposits are present in the sedimentary rocks of the SHR basin (Chough et al., 2000), SO_4^{2-} increases abruptly as waters flow through sedimentary rocks (Fig. 4). This may be attributed to the impacts of increased agricultural discharge in the downstream rural areas or oxidation of disseminated sulfide minerals in coalfields and abandoned polymetallic skarn deposits within the sedimentary basin.

Water—rock interaction

On the TDS vs. $Na^+/(Na^+ + Ca^{2+})$ diagram (Fig. 5), the SHR data plot within the rock dominance field, similar to the Chinese rivers (Gaillardet et al., 1999; Han and Liu, 2004), while the NHR data are marked around the boundary between the fields of rock dominance and precipitation, similar to the Amazon and the Niger rivers (Gibbs, 1970). These

data indicate rock weathering for the SHR and atmospheric input for the NHR as the dominant controls on their hydrochemistry. A few samples from the SHR (S-1) and the NHR (NS-1 and NS-2) are marked off the major groupings, in the field of precipitation dominance (Fig. 5). These samples were collected from the pristine headwaters draining granitic terrains. Such observation indicates atmospheric input as the main factor controlling the chemistry of these waters.

The Ca^{2+}, Mg^{2+} and HCO_3^- concentrations are much higher in the SHR than in the NHR (Table 1). Downriver increase in these ions in the SHR is also observed and is attributed to weathering of calcite and dolomite in the watershed. According to the mineral stability diagram (not shown), the NHR water is in equilibrium with kaolinite. However, in the headwaters of the SHR, water seems to be in equilibrium with carbonate minerals first, then with gibbsite, and finally with kaolinite.

Oxygen and hydrogen isotopes

Oxygen and hydrogen isotopes vary from −11.7 to −8.9‰ and from −80 to −66‰, respectively (Fig. 6a). Seasonal variations of the two isotopes are shown in Fig. 6b. On the δD vs. $\delta^{18}O$ diagram, most water samples plot close to the
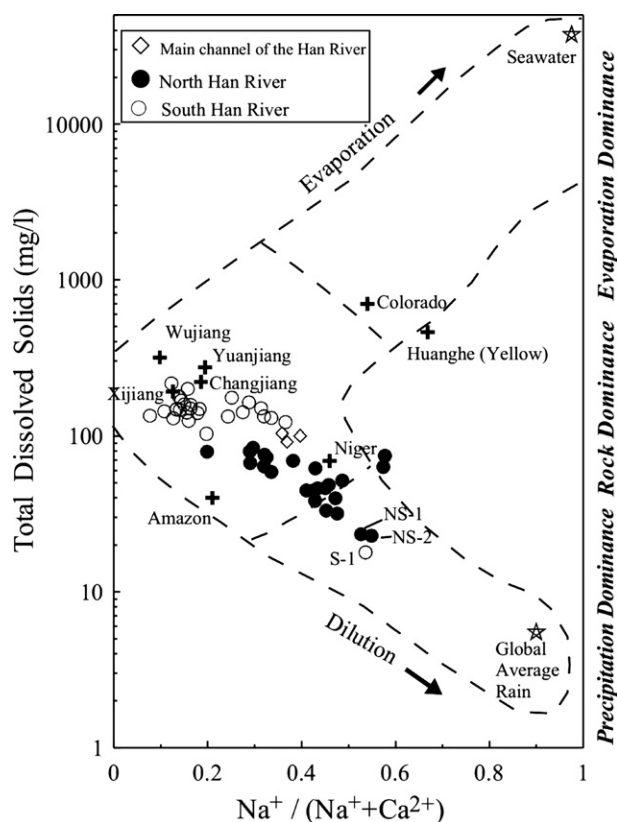

Figure 5 Plot of TDS vs. $Na^+/(Na^+ + Ca^{2+})$ (after Gibbs, 1970). Most of the South Han River data plot in the rock dominance field similar to the Chinese rivers (Gaillardet et al., 1999; Han and Liu, 2004), whereas the North Han River data plot around the boundary between rock dominance and precipitation dominance fields.

global meteoric water line (Craig, 1961). Summer samples collected from the reservoirs (dams) are enriched in heavier isotopes and slightly off from the local meteoric water line (LMWL; Lee and Lee, 1999). They appear to have undergone variable degrees of evaporation. Evaporation line is defined with a slope of 5.58 (n = 12; r^2 = 0.99), significantly less than that of LMWL (8.05).

According to Gonfiantini (1986), percentage of evaporation loss of waters can be calculated: $x = \frac{(\delta_S - \delta_I)(1 - h + \Delta\varepsilon)}{(\delta_S + 1)(\Delta\varepsilon + \varepsilon/\alpha) + h(\delta_a - \delta_S)}$, where x is the percentage of evaporation loss with respective to the total water input into the basin. δ_S is the mean isotopic composition of the summer Han River samples. δ_I is the mean isotopic composition of the input to the Han River which was obtained from the interception of the regression line for summer river samples and the LMWL of Lee and Chung (1997) (refer to Fig. 6). δ_a is the mean isotopic composition of water vapor calculated assuming an isotopic equilibrium with local precipitation ($\delta_a = \delta_I - \varepsilon^*$, where $\varepsilon^* = 1000 \times (\alpha - 1)$ and $\varepsilon = \alpha - 1$): (Lee and Veizer, 2003).
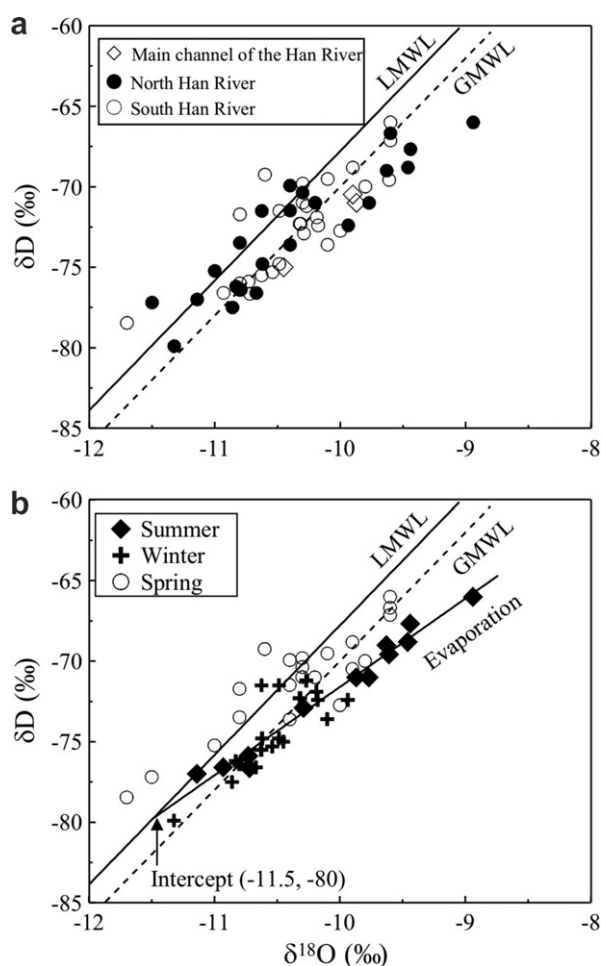

Figure 6 Plot of δD vs. $\delta^{18}O$ values of river water samples. Stable isotopic compositions vary as a function of geographic location (a), as well as seasonally (b). Summer samples are enriched in their heavy isotopic compositions due to evaporation. Local meteoric water line (LMWL) and global meteoric water line (GMWL) are from Lee and Chung (1997) and Craig (1961), respectively.

The relative humidity (h) is assumed as 0.79 based on the meterological data of the study area (Korea Meteorological Administration, http://www.kma.go.kr). α is the equilibrium fractionation factor for oxygen isotopes (ln α = 1137 T^{-2} − 0.4156 T^{-1} − 0.00207) and hydrogen isotopes (ln α = 24844 T^{-2} − 76.248 T^{-1} + 0.05261) (Friedman and O'Neil, 1997). For the α calculation, we used the average temperature of river water collected during the summer. $\Delta\varepsilon$ is the kinetic enrichment factor for oxygen isotopes (14.2 × (1 − h)) and for hydrogen isotopes (12.5 × (1 − h)) (Gonfiantini, 1986).

Water lost by evaporation during summer season is estimated as 13.3 ± 1.5% and 7.2 ± 1.1% of total precipitation input into the reservoirs of the NHR and SHR basins, respectively, in which the potential errors of evaporative loss estimates are evaluated through consideration of possible variations in basin storage, humidity, and the isotopic composition of atmospheric vapor (Gibson et al., 1993).

The reason for higher evaporation loss in the NHR than in the SHR is probably due to the impact of several flood control dams in the NHR basin. There are six dams on the NHR compared to only one on the SHR (Fig. 1). Similar observations have been reported from dammed rivers elsewhere (Clark and Fritz, 1997).

Sulfur isotopes

Sources of dissolved SO_4^{2-} in natural river waters may include dissolution of sedimentary sulfates, oxidation of both sulfide minerals and organic materials, and anthropogenic inputs (Thode, 1991; Grasby et al., 1997). Various geochemical tools can be used as tracers for identifying sources of SO_4^{2-} waters. Of these, sulfur isotopic signature of SO_4^{2-} is most diagnostic. For example, SO_4^{2-} from dissolution of marine evaporates such as gypsum/anhydrite has $\delta^{34}S$ values ranging from 10 to 30‰ with an average of ~20‰ (Claypool et al., 1980), while sulfides from igneous rocks have $\delta^{34}S$ values ranging from −10 to 10‰ with an average of ~0‰ (Thode, 1991). Sedimentary sulfides are characterized by negative $\delta^{34}S$ values (Thode, 1991), and precipitation from anthropogenic sources has $\delta^{34}S$ values ranging from 4 to 6‰ (Caron et al., 1986; Mcardle and Liss, 1995; Wadleigh et al., 1996).

Fig. 7 shows sulfate concentrations and $\delta^{34}S_{SO_4}$ values obtained from the Han River. Because the NHR basin consists entirely of basement gneiss and granite with no sedimentary rocks, the possible sources of sulfates in the river water can be assumed to be atmospheric input and oxidation of sulfide minerals in silicate rocks. However, according to Yu and Park (2004), metamorphic rocks in the study area contain little sulfides, exerting little impact on sulfate concentration in the river water. They reported SO_4^{2-} in the range of 0.01 and 0.15 mmol/l and $\delta^{34}S_{SO_4}$ values in the range of 3.9 and 8.2‰ for rain samples collected from the city of Chuncheon located in the northeastern part of the NHR basin (Figs. 1 and 7). Based on sulfur isotopes and the result of factor analysis, they argued that atmospheric input could be the major contributor of sulfate in the NHR basin. On the chloride vs. sulfate diagram (Fig. 7a), the NHR data plot close to the precipitation data from Yu and Park (2004), indicating an atmospheric origin. In addition, our relatively
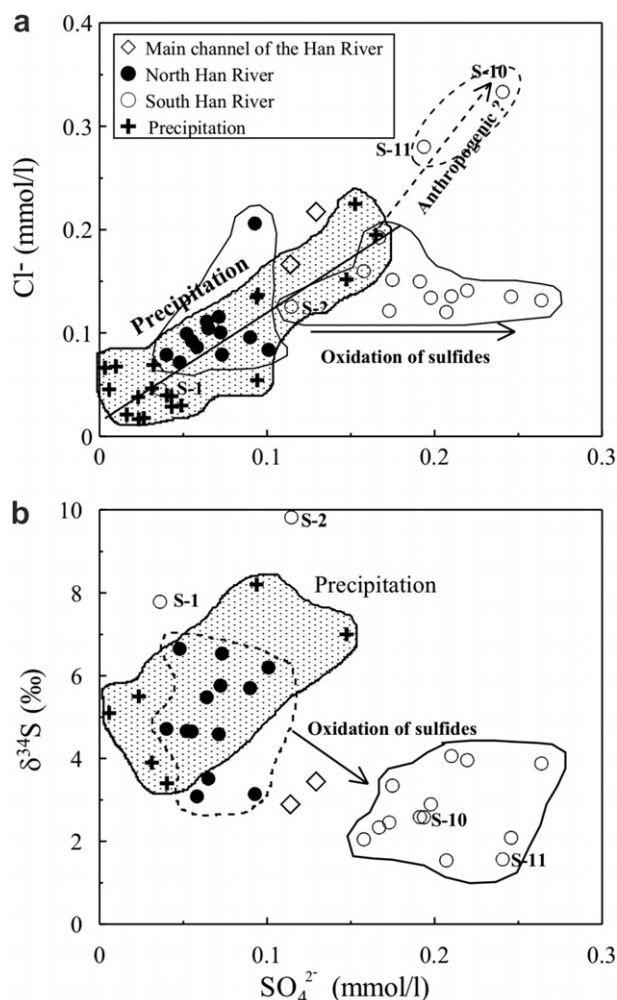
Figure 7 Plot of Cl vs. SO_4^{2-} concentrations (a), $\delta^{34}S$ vs. SO_4^{2-} concentrations (b) of river water samples. The cross symbols and dotted area represent data of precipitation obtained by Yu and Park (2004). In the North Han River basin, SO_4^{2-} sources are mostly related to deposition of atmospheric sulfates, while in the South Han River basin, they are closely related to oxidation of sulfide minerals as well as deposition of atmospheric sulfates.

low SO_4^{2-} concentration (mean = 0.06 ± 0.02 mmol/l, n = 25) and high $\delta^{34}S_{SO_4}$ values (3.1–6.7‰, mean = 5.0 ± 1.2‰, n = 13) resemble sulfates from atmospheric sources in the Indus basin (e.g. Karim and Veizer, 2000).

Most of $\delta^{34}S_{SO_4}$ data in the SHR presented in Fig. 7a deviate significantly from the precipitation data from Yu and Park (2004), suggesting contributions from other sources of sulfates in the river water. As discussed in Section ''Seasonal and spatial variations in water chemistry'', relatively high SO_4^{2-} (mean = 0.20 ± 0.07 mmol/l, n = 27) and low $\delta^{34}S_{SO_4}$ values (1.6–9.8‰, mean = 3.5 ± 2.2‰, n = 15) in the SHR could be attributed to oxidation of sulfides in the abandoned polymetallic deposits and coal-bearing sedimentary rocks in the headwaters.

Two water samples (S-1 and S-2) collected from the headwaters of the SHR basin plot close to the NHR data, indicating atmospheric input of sulfates (Fig. 7b). The

$\delta^{34}S_{SO_4}$ values of acid drainage from a coal mine located in the northeastern Gangwon Province were estimated as 1.1–1.8‰ by Yu and Coleman (2000). The $\delta^{34}S_{SO_4}$ values of the SHR (3.2 ± 2.2‰) correspond to the average $\delta^{34}S_{SO_4}$ values (3.6 ± 2.3‰) between rainfall and acid mine drainage, indicating a mixture of these two sources. Two river samples (S-10 and S-11) taken from near the Paldang dam are distinctly enriched in chloride concentrations and significantly deviate from the major grouping of the Han River waters (Fig. 7a). These samples may be affected by anthropogenic contamination, as indicated by increased chloride and nitrate concentrations.

Strontium isotopes

Generally, Sr isotopic compositions of river water are similar to those of the parent rocks of their drainage basin because Sr isotopes are not fractionated during weathering processes for carbonate, evaporite and basalt (Faure, 1986). Hence, Sr isotopes have been used as powerful tool for identifying sources of dissolved loads in river waters (Négrel and Dupré, 1995; Zhang et al., 1995; Gaillardet et al., 1997; Viers et al., 2000; Quade et al., 2003). In addition, Sr behaves conservatively during mixing. Négrel and Dupré (1995) used Sr isotopes for delineating mixing of different water bodies originating from different rock types in some streams in Central Africa.

Mean Sr concentrations are approximately three times higher in the SHR (1.49 ± 0.65 μmol/l, n = 27) than in the NHR (0.53 ± 0.17 μmol/l, n = 25), while the $^{87}Sr/^{86}Sr$ ratios are lower in the SHR (0.71495–0.71785, mean = 0.71622, excluding one sample S-1) than in the NHR (0.71793–0.72722, mean = 0.72278). Sample S-1 taken from the headwaters of the SHR basin shows similar $^{87}Sr/^{86}Sr$ value (0.73209) as the NHR, indicating granitic source for Sr.

On the $^{87}Sr/^{86}Sr$ vs. 1000 Sr/Na diagram (Fig. 8), all water samples from the Han River plot between two end-members, i.e. silicates in the NHR basin and carbonates in the SHR basin. The first end-member can be characterized by low $^{87}Sr/^{86}Sr$ ratio associated with the highest Sr content, probably originating from carbonate rocks distributed in the northeastern part of the SHR basin (Kwon et al., 1991). The second end-member can be characterized by high $^{87}Sr/^{86}Sr$ ratio associated with the lowest Sr content, probably derived from Precambrian gneisses and Mesozoic granites (Kim et al., 1997). Sample NS-1 taken from a tributary in the upper basin of the NHR is characterized by much lower Sr content and lower $^{87}Sr/^{86}Sr$ ratio than other NHR samples (Fig. 8), indicating geological heterogeneity in the tributary. Further detailed investigation on the geology and Sr isotopic compositions of the tributary is warranted.

Quantifying mixing of river waters at confluence point

Kim et al. (2002) showed that stream flows in an effluent-dominated stream could be estimated using various solutes in the effluents. Their flow data estimated using solutes as tracers were in good agreement with the physical measurement data. Utilization of solutes as natural tracers may pro-
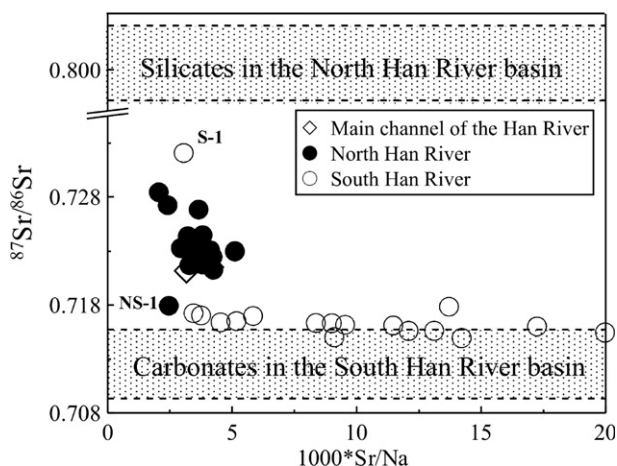
Figure 8 Plot of $^{87}Sr/^{86}Sr$ vs. $1000 \times Sr/Na$. The $^{87}Sr/^{86}Sr$ ratios in the North Han River are much higher than those in the South Han River, reflecting differences in isotopic composition of weathered rocks.

vide time- and cost-effective approach for estimating flows. They eliminate the needs for injection of artificial tracers and allow use of simple potable conductivity meters for on-site measurements.

For this study, mixing ratios of the NHR and SHR waters at the Paldang dam are estimated using a two-component mass-balance model employing solutes and isotopes as natural tracers. Generally, mixing models using natural tracers can be reliable if the tracers are conservative and their sources are well defined. When using tracers for estimating stream flows, it is generally assumed that compositions of the resulting mixtures are not modified by chemical reactions or physical processes. Various solutes (e.g., Sr^{2+}, Mg^{2+}, Cl^- and SO_4^{2-}) and isotopes (e.g., $^{87}Sr/^{86}Sr$, $\delta^{18}O$ and δD) have been used as natural tracers for quantifying mixing of water via end-member mixing analyses (e.g., Faure, 1986; Eikenberg et al., 2001; Kim et al., 2002). Ideally, a reliable two-component isotope system would yield data points for mixed samples marked on a straight line connecting both end-members (e.g., Faure, 1986; Eikenberg et al., 2001).

Mixing ratios of each river component at the confluence can be estimated using the following two-component mass-balance model:

$$Q_M = Q_N + Q_S \qquad (1)$$
$$Q_M C_M = C_N Q_N + C_S Q_S \qquad (2)$$

where 'Q' and 'C' denote stream flow and concentration of a conservative tracer, respectively; and subscripts 'M', 'N' and 'S' denote the main channel of the Han River, NHR, and SHR, respectively.

Utilizing Sr isotopic ratios and Sr contents as tracers, it is estimated that the Paldang reservoir water (sample M-1) consists of 38% of the SHR water and 62% of the NHR water in the summer (August 2000), and 35% of the SHR water and 65% of the NHR water in the early spring (March 2001). On the other hand, when Mg^{2+} and SO_4^{2-} are used as tracers, it is estimated that the Paldang reservoir water (sample M-1) consists of 39% of the SHR water and 61% of the NHR water in the summer (August 2000), and 25% of

the SHR water and 75% of the NHR water in the early spring (March, 2001). Noticeably, mixing ratios estimated using solute concentrations as tracers are in good agreement with those estimated using isotopes as tracers for the summer samples, indicating conservative behavior of all tracers. However, there is a slight difference (~10%) between the mixing ratios estimated for the spring samples when using chemical and isotope tracers. This discrepancy may be attributed to incomplete mixing of waters or contribution from other sources, for example, input of anthropogenic contaminants (e.g., fertilizer, manure, sewage, road salt).

Conclusions

This study indicates that hydrochemistry of the Han River is mainly controlled by rock weathering, i.e. silicates in the NHR basin and carbonates in the SHR basin. The NHR is characterized by low concentrations of TDS, major ions, and Sr, but high concentrations of Si, high values of $\delta^{34}S_{SO_4}$ and $^{87}Sr/^{86}Sr$ ratios, while the SHR exhibits contrasting characteristics. Seasonal variations in water chemistry are primarily related to variations in river discharge. In the headwaters solute concentrations are high during low flow (winter) but diluted by summer floods. The $\delta^{18}O$ and δD compositions are heavier in the summer, indicating increased evaporation in the reservoirs caused by higher temperatures during summer. Deposition of atmospheric sulfates is the major source for sulfates in the NHR basin, while oxidation of sulfide minerals plus atmospheric deposition contribute to sulfates in the SHR. Low Sr concentrations, but high $^{87}Sr/^{86}Sr$ in the NHR and high Sr concentrations, but low $^{87}Sr/^{86}Sr$ in the SHR reflect silicate and carbonate weathering, respectively. Mixing calculation based on Sr isotopes and $Mg^{2+} - SO_4^{2-}$ reveals 61–75% of the NHR waters at confluence point.

Acknowledgements

References

Amiotte-Suchet, P., Probst, J.L., 1993. Modelling of atmospheric CO_2 consumption by chemical weathering of rocks: application to the Garonne, Congo and Amazon basins. Chemical Geology 107, 205–210.

Caron, F., Tessier, A., Kramer, J.R., Schwarcz, H.P., Rees, C.E., 1986. Sulphur and oxygen isotopes of sulfate in precipitation and lake water, Quebec. Applied Geochemistry 1, 601–606.

Chae, K.T., Yun, S.T., Kim, K.H., Lee, P.K., Choi, B.Y., 2004. Atmospheric versus lithogenic contribution to the composition of first- and second-order stream waters in Seoul and its vicinity. Environmental International 30, 73–85.

Chough, S.K., Kwon, S.-T., Ree, J.H., Choi, D.K., 2000. Tectonic and sedimentary evolution of the Korean peninsula: a review and new review. Earth-Science Reviews 52, 175—235.

Clark, I.D., Fritz, P., 1997. Environmental Isotopes in Hydrogeology. Lewis Publishers, New York, USA, p. 328.

Claypool, G.E., Holser, W.T., Kaplan, I.R., Sakai, H., Zak, I., 1980. The age curve of sulfur and oxygen isotopes in marine sulfates and their mutual interpretation. Chemical Geology 28, 199—260.

Coleman, M.L., Shepherd, T.J., Durham, J.J., Rouse, J.E., Moore, G.R., 1982. Reduction of water with zinc for hydrogen isotope analysis. Analytical Chemistry 54, 993—995.

Craig, H., 1961. Isotopic variations in meteoric waters. Science 133, 1702—1703.

Eikenberg, J., Tricca, A., Vezzu, G., Stille, P., Bajo, S., Ruethi, M., 2001. $^{228}Ra/^{226}Ra/^{224}Ra$ and $^{87}Sr/^{86}Sr$ isotope relationships for determining interactions between ground and river waters in the upper Rhine valley. Journal of Environmental Radioactivity 54, 133—162.

Epstein, S., Mayeda, T.K., 1953. Variation of ^{18}O content of waters from natural sources. Geochimica et Cosmochimica Acta 4, 213—224.

Faure, G., 1986. Principles of Isotopes Geology. John Wiley and Sons, New York, p. 897.

Friedman, I., O'Neil, J.R., 1997. Compilation of stable isotope fractionation factors of geochemical interest. In: Data of Geochemistry, sixth ed., Geol. Surv. Prof. Pap. 440-KK, US, Govt. Print. Off., Washington, D.C.

Gaillardet, J., Dupré, B., Allègre, C.J., Négrel, P., 1997. Chemical and physical denudation in the Amazon River basin. Chemical Geology 142, 141—173.

Gaillardet, J., Dupré, B., Louvat, P., Allègre, C.J., 1999. Global silicate weathering and CO_2 consumption rates deduced from the chemistry of large rivers. Chemical Geology 159, 3—30.

Gibbs, R.J., 1970. Mechanisms controlling world water chemistry. Science 17, 1088—1090.

Gibson, J.J., Edwards, T.W.D., Bursey, G.G., Prowse, T.D., 1993. Estimating evaporation using stable isotopes: quantitative results and sensitivity analysis for two catchments in northern Canada. Nordic Hydrology 24, 79—94.

Gonfiantini, R., 1986. Environmental isotopes in lake studies. In: Fritz, P., Fontes, J.Ch. (Eds.), Handbook of Environmental Isotope Geochemistry, vol. 2. Elsevier, New York, pp. 113—168.

Grasby, S.E., Hutcheon, I., Krouse, H.R., 1997. Application of the stable isotope composition of SO_4 to tracing anomalous TDS in Nose Creek, southern Alberta, Canada. Applied Geochemistry 12, 567—575.

Han, G., Liu, C.Q., 2004. Water geochemistry controlled by carbonate dissolution: a study of the river waters draining karst-dominated terrain, Guizhou Province, China. Chemical Geology 204, 1—21.

Huh, Y., Tsoi, M.Y., Zaitsev, A., Edmond, J.M., 1998. The fluvial geochemistry of the rivers of Eastern Siberia I: Tributaries of the Lena River draining the sedimentary platform of the Siberian Craton. Geochimica et Cosmochimica Acta 62, 1657—1676.

Karim, A., Veizer, J., 2000. Weathering processes in the Indus River Basin: implications from riverine carbon, sulfur, oxygen, and strontium isotopes. Chemical Geology 170, 153—177.

Kim, J.H., Cheong, C.S., Son, Y.C., Koh, H.J., 1997. Geology and Sr, Nd and Pb isotopic compositions of Precambrian granitoids in the Pyeongchang area, Korea. Journal of Geological Society of Korea 33, 27—35, in Korean with English abstract.

Kim, K., Lee, J.S., Oh, C.W., Hwang, G.S., Kim, J., Yeo, S., Kim, Y., Park, S., 2002. Inorganic chemicals in an effluent-dominated stream as indicators for chemical reactions and streamflows. Journal of Hydrology 264, 147—156.

KOWACO, 1993. The pre-investigation report for groundwater resources. Korea Water Resources Corporation, p. 340 (in Korean).

Kwon, S.T., Lee, H.Y., Lam, C.Y., Lee, B.S., Suh, K.S., Do, S.J., 1991. Preliminary Sr-Nd isotopic study of Lower Paleozoic carbonat rocks and Conodonts, Korea. Journal of Geological Society of Korea 27, 587—596, in Korean with English abstract.

Lee, K.S., Chung, J.I., 1997. Stable isotopic variation of precipitation in Pohang, Korea. Korea Society of Economic and Environmental Geology 30, 321—325, in Korean with English abstract.

Lee, K.S., Kim, Y., 2007. Determining the seasonality of groundwater recharge using oxygen and hydrogen isotopes: a case study from the upper North Han River basin, Korea. Environmental Geology 52, 853—859.

Lee, K.S., Lee, C.B., 1999. Oxygen and hydrogen isotopic composition of precipitation and river waters in South Korea. Journal of Geological Society of Korea 35, 73—84, in Korean with English abstract.

Lee, D., Veizer, J., 2003. Water and carbon cycles in the Mississippi River basin: Potential implications for the Northern Hemisphere residual terrestrial sink. Global Biogeochemical Cycles 17, 1037. doi:10.1029/2002GB001984.

Lee, K.S., Ryu, J.S., Ahn, K.H., Chang, H.W., Lee, D., 2007. Factors controlling carbon isotope ratios of dissolved inorganic carbon in two major tributaries of the Han River, Korea. Hydrological Processes 21, 500—509.

Mcardle, N.C., Liss, P.S., 1995. Isotopes and atmospheric sulphur. Atmospheric Environment 29, 2553—2556.

Meybeck, M., 1983. Atmospheric inputs and river transport of dissolved substances. Proceedings of the Hamburg Symposium, IAHS Publ. 141, 171—192.

Meybeck, M., 1988. Global chemical weathering from surficial rocks estimated from river dissolved loads. American Journal of Science 287, 401—428.

Mizutani, Y., Nakai, N., Hong, S.O., 1982. Geochemical studies on the principal dissolved chemical component in Han River. Korean Journal of Limnology 15, 1—6.

Moon, S., Huh, Y., Qin, J., van Pho, N., 2006. Chemical weathering in the Hong (Red) River basin: Rates of silicate weathering and their controlling factors. Geochimica et Cosmochimica Acta 71, 1411—1430.

Négrel, Ph., Dupré, B., 1995. Temporal variations in Sr isotopic ratios, major and trace element composition of the Oubangui river basin: implication for the sources of material. In: Oliver, J.C., Boulegue, J. (Eds.), Colloque Grands Bassins Fluviaux peri Atlantiques: Congo, Niger, Amazone. 22—24 November 1993. ORSTOM, CNRS, INSU, Paris, pp. 39-50.

Petelet, E., Luck, J.M., Othman, D.B., Négrel, P., Aquilina, L., 1998. Geochemistry and water dynamics of a medium-sized watershed: the Hérault, southern France: 1. Organization of the different water reservoirs as constrained by Sr isotopes, major, and trace elements. Chemical Geology 150, 63—83.

Qin, J., Huh, Y., Edmond, J.M., Du, G., Ran, J., 2006. Chemical and physical weathering in the Min Jiang, a headwater tributary of the Yangtze River. Chemical Geology 227, 53—69.

Quade, J., English, N., DeCelles, P.G., 2003. Silicate versus carbonate weathering in the Himalaya: a comparison of the Arun and Seti River watersheds. Chemical Geology 202, 275—296.

Stallard, R.F., Edmond, J.M., 1981. Geochemistry of the Amazon: I. Precipitation chemistry and the marine contribution to the dissolved load at the time of the peak discharge. Journal of Geophysical Research 86, 9844—9858.

Stallard, R.F., Edmond, J.M., 1987. Geochemistry of the Amazon: 3. Weathering chemistry and limits to dissolved inputs. Journal of Geophysical Research 92, 8293—8302.

Thode, H.G., 1991. Sulfur isotopes in Nature and the environment: an overview. In: Krouse, H.R., Grinenko, V.A. (Eds.), Stable Isotopes: Natural and Anthropogenic Sulphur in the Environment. SCOPE 43. John Wiley and Sons, pp. 1—26.

Vedula, S., Medina, F., 2002. Comparing the in stream and out stream water quality of Kennewick irrigation district. In: Proceedings of the Research and Extension Regional Water Quality Conference 2002, pp.1—3.

Viers, J., Dupré, B., Braun, J.J., Deberdt, S., Angeletti, B., Ngoupayou, J.N., Michard, A., 2000. Major and trace element abundances, and strontium isotopes in the Nyong basin rivers (Cameroon): constraints on chemical weathering procedures and elements transport mechanisms in humid tropical environments. Chemical Geology 169, 211—241.

Wadleigh, M.A., Schwarcz, H.P., Kramer, J.R., 1996. Isotopic evidence for the origin of sulfate in coastal rain. Tellus 48B, 44—59.

Wu, L., Huh, Y., Qin, J., Du, G., van Der Lee, S., 2005. Chemical weathering in the Upper Huang He (Yellow River) draining the eastern Qinghai-Tibet Plateau. Geochimica et Cosmochimica Acta 69, 5279—5294.

Xu, Z., Liu, C.Q., 2007. Chemical weathering in the upper reaches of Xijiang River draining the Yunnan—Guizhou Plateau, Southwest China. Chemical Geology.

Yanagisawa, F., Sakai, H., 1983. Thermal decomposition of barium sulfate-vanadium pentoxide-silica glass mixture for preparation of sulfur dioxide in sulfur isotope ratio measurements. Analytical Chemistry 55, 985—987.

Yu, J.Y., Coleman, M., 2000. Isotopic compositions of dissolved sulfur in acid mine drainages: case study on Youngdong and Gangreung coal mines, Korea. Journal of Geological Society of Korea 36, 1—10, in Korean with English abstract.

Yu, J.Y., Park, Y., 2004. Sulphur isotopic and chemical compositions of the natural waters in Chuncheon area, Korea. Applied Geochemistry 19, 843—853.

Yu, J.Y., Choi, I.K., Kim, H.S., 1994. Geochemical characteristics of the surface water depending on the bed rock types in the Chuncheon area. Journal of Geological Society of Korea 30, 307—324, in Korean with English abstract.

Zhang, J., Takahashi, K., Wushiki, H., Yabuki, S., Xiong, J.M., Masuda, A., 1995. Water geochemistry of the rivers around the Taklimakan Desert (NW China): Crustal weathering and evaporation processes in arid land. Chemical Geology 119, 225—237.